Hunting for microseismic reflections using multiplets

Noha S. Farghal and Stewart A. Levin

ABSTRACT

Microseismic monitoring of hydraulic fracturing is often used to locate reactivated faults and newly created fractures by locating the microseismic sources that occur during the process. These microseisms generate reflections as well as direct arrivals, but they tend to be fairly weak and quite difficult to locate and image. In this work we identify multiplets, i.e. repeated microseisms originating from about the same subsurface location, and thereby identify their consistent reflections.

INTRODUCTION

Hydraulic fracturing is routinely used to increase production rates from unconventional resources such as tight sands and shale plays. Its effectiveness depends largely on the geometry of the induced fractures. Microseismic monitoring is often used to assess this geometry by picking these earthquake-like arrivals and locating their sources along the fractures.

Microseismic recordings also contain reflected arrivals that may be useful for imaging the reservoir (Asanuma et al., 2011; Tamakawa et al., 2010; Reshetnikov et al., 2009). However, due to their small magnitudes, such reflections may not be easy to identify on a seismogram. In this work we key on the frequent presence of repeated events known as multiplets that originate from about the same subsurface location and have nearly identical source characteristics. Our assumption is that they must also generate nearly identical reflections. By extracting, aligning and stacking these events we reduce background noise and enhance both the direct arrivals and the weaker reflections that follow them.

Our aim for reflection identification is to use these high frequency deep sources to image the subsurface. Although such a use of microseismic sources has been done before in subsurface imaging (Asanuma et al., 2011; Tamakawa et al., 2010; Reshetnikov et al., 2009), to the best of our knowledge none of these sources were hydraulically induced.

METHOD

To identify multiplets in seismograms, we adapt a method from earthquake seismology which involves identifying clear direct arrivals (master waveforms), performing normalized cross-correlations of them with the microseismic recordings taken during the treatment, and thresholding the peak correlations to identify and group arrivals into multiplets (Brown et al., 2008; Eisner et al., 2008; Shelly et al., 2011).

We assessed the peak on the average correlations across all the 36 channels in each cross-correlation record. To accommodate small differences in source locations within each multiplet, we tested two positive and two negative receiver linear moveouts and chose the moveout yielding the highest peak cross-correlation. We used the peak magnitude to decide whether the record was part of a multiplet and, if so, the peak location was used for subsequent alignment and stacking of the records in the multiplet.

APPLICATION

The dataset we used in this work was obtained from a monitoring well in the Bossier play (a shale and sand gas reservoir) located in the Dowdy Ranch Field, Texas. The data were collected before (background) and during hydraulic fracture treatments with an array of 12 three-component geophones in a monitoring well. The well was 500ft away from the treatment well (Sharma et al., 2008). The data used in this report are from hydraulic fracture treatment of the Bonner sand formation in this field.

A sonic log has been supplied to us with the data to aid interpretations. As can be seen on Figure 1, there are a couple of strong velocity contrasts that could produce moderately strong reflections.

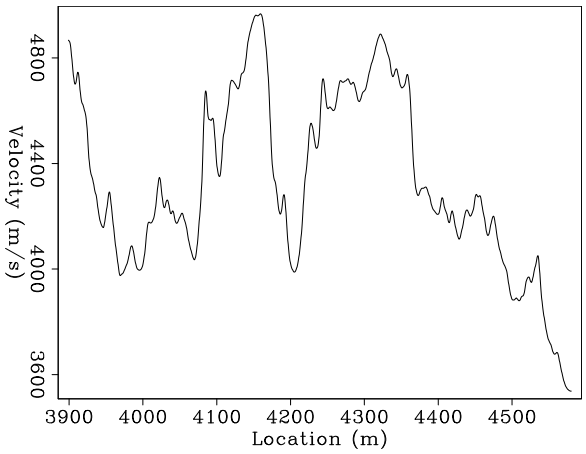

Figure 1: Velocity from a sonic log in the monitoring well. [**ER**]

Figure 2 shows a seismogram used for the generation of a master waveform. The waveform between 0.14 and 0.19 s (Figure 3) was extracted from the original seismogram. Normalized cross-correlations of this master waveform with other 0.5 s event

windows in the dataset was performed. An example cross-correlation peak of the master with the event window from which it was obtained is shown in Figure 4. The stacked cross-correlation of the peak shown in Figure 4 can be seen in Figure 6(a).

The correlation of the master with another event window is shown in Figure 5. The correlation is stacked (Fig. 6(b)), and the peak location used as detailed below to align this record with that from which the master was extracted.

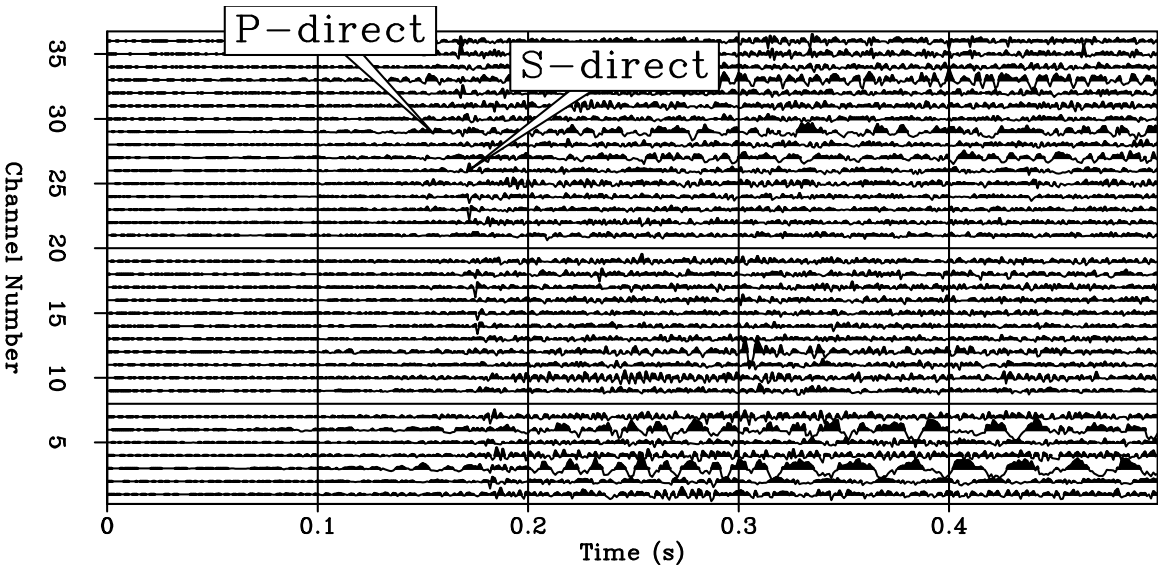

Figure 2: Seismogram used in the generation of the master waveform in Figure 3, showing both P and S arrivals. [**ER**]

We used the magnitude of the background correlation of Figures 4 and 5 to set our threshold (minimum) cross-correlation value for multiplet detection. Events that had cross-correlation magnitudes equal to or exceeding this threshold were considered matches/multiplets and used for alignment and stacking. By alignment, we mean that matching waveforms are shifted so that, within the 0.5s event windows they are in, they occur at the same temporal location. This was achieved by applying a bulk positive or negative shift to each event window. The shift for each event window containing a multiplet was the difference in temporal location of the master waveform location and the location of the cross-correlation peak rounded to the nearest sample. After alignment the events were summed together, as shown in Figure 7.

Figure 7 shows stacked traces for the master taken from the seismogram shown in Figure 2. It is clear on the stacked event that the main waveform is followed by another wavelet around 0.39s that was not apparent in the original file from which the master waveform was taken. The event did show up almost consistently at the same temporal offset in most events in the multiplet used to generate this stacked event, as shown in Figures 8–11.

We performed singular value polarization analysis for this stack of events (see the appendix for details) and used this information to emphasize reflection type (S or P).

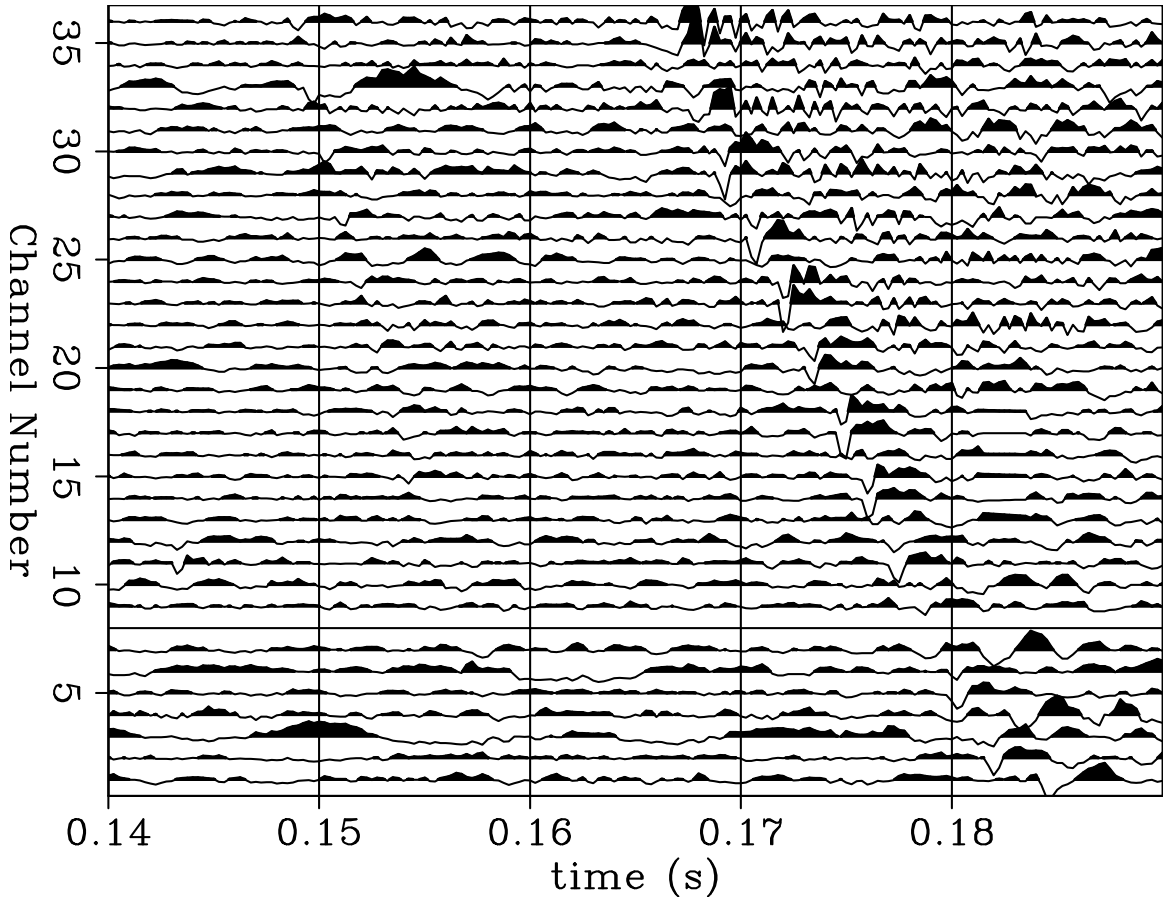

Figure 3: Master waveform extracted from Figure 2 by windowing in time around 0.14 and 0.19 s. [**ER**]

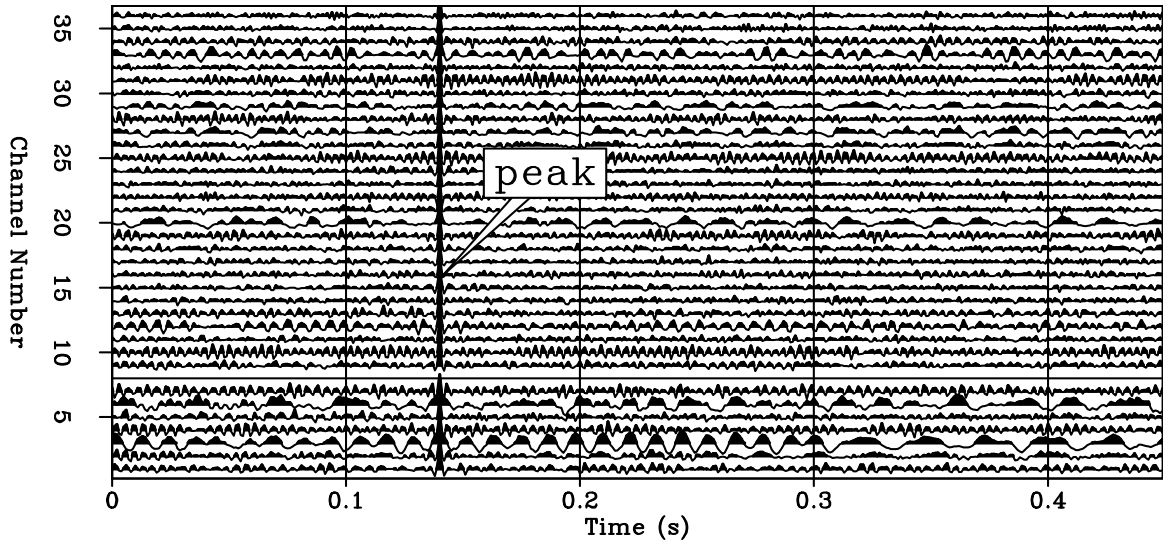

Figure 4: Cross-correlation of the master with its original event window (Figure 2).The correlation peak is marked [**ER**]

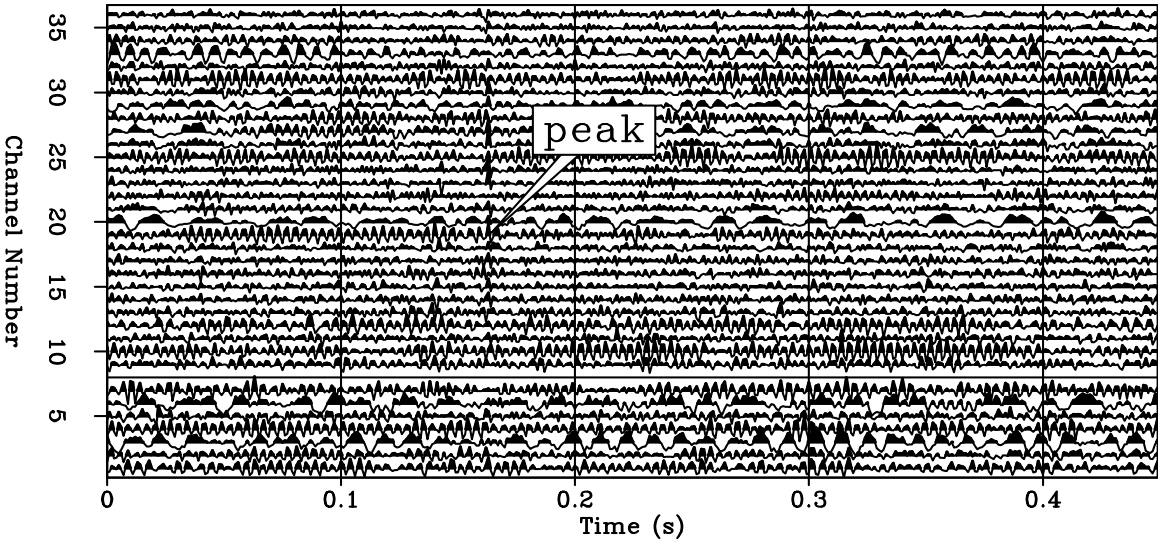

Figure 5: Cross-correlation of the master with another event window with the correlation peak marked [**ER**]

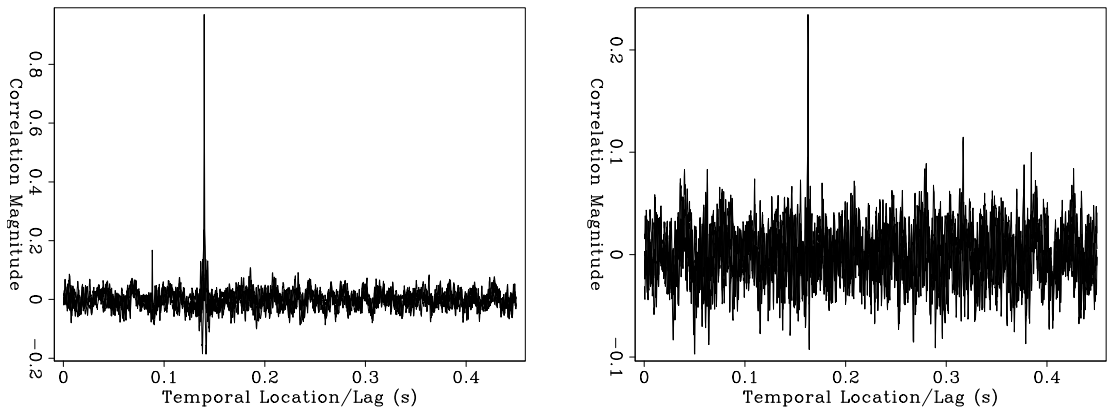

(a) (b)

Figure 6: a) Stack of the correlation in Figure 4. The peak correlation value of 1 reflects the fact that the master window was extracted from the same record. b) Stack of the correlation in Figure 5. Here the peak correlation of 0.24 stands out above the background level of 0.05–0.1. [**ER**]

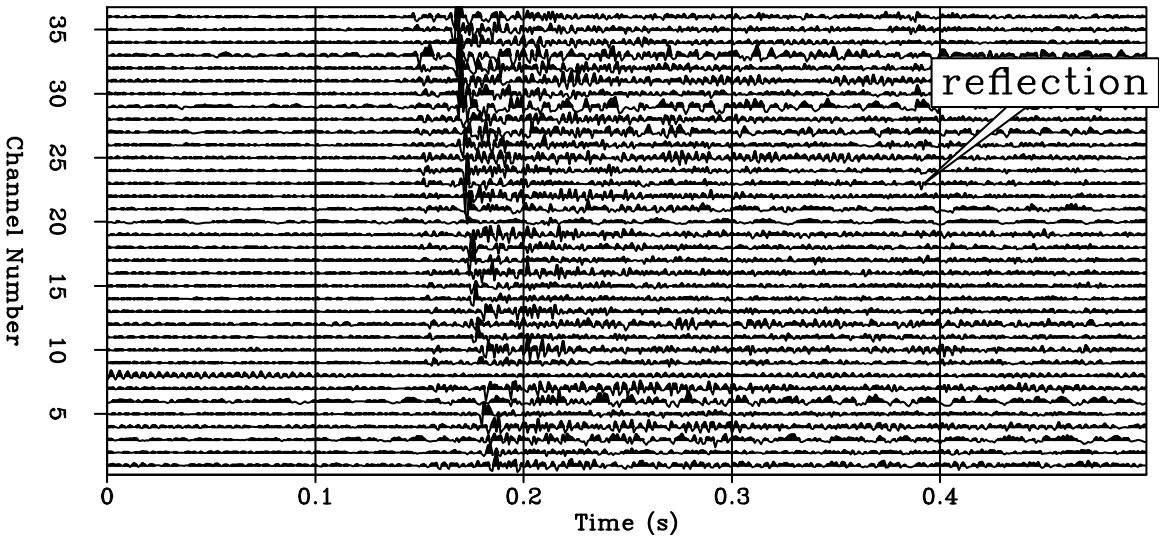

Figure 7: Stacked multiplets for the waveform in Figure 2 with the S reflection marked. [**ER**]

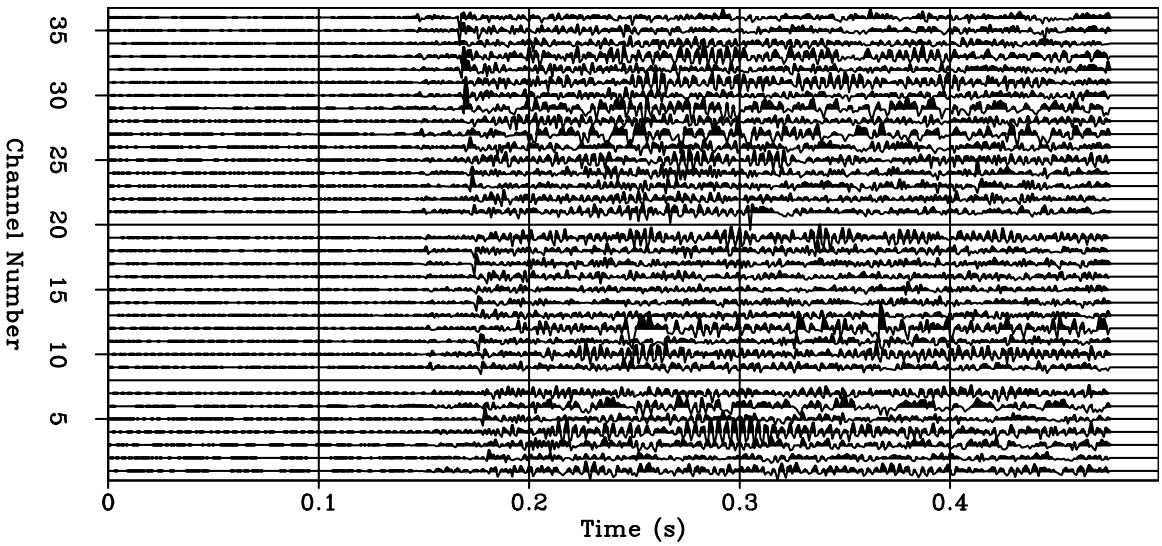

Figure 8: One of the seismograms used in making the stack in Figure 7. [**ER**]

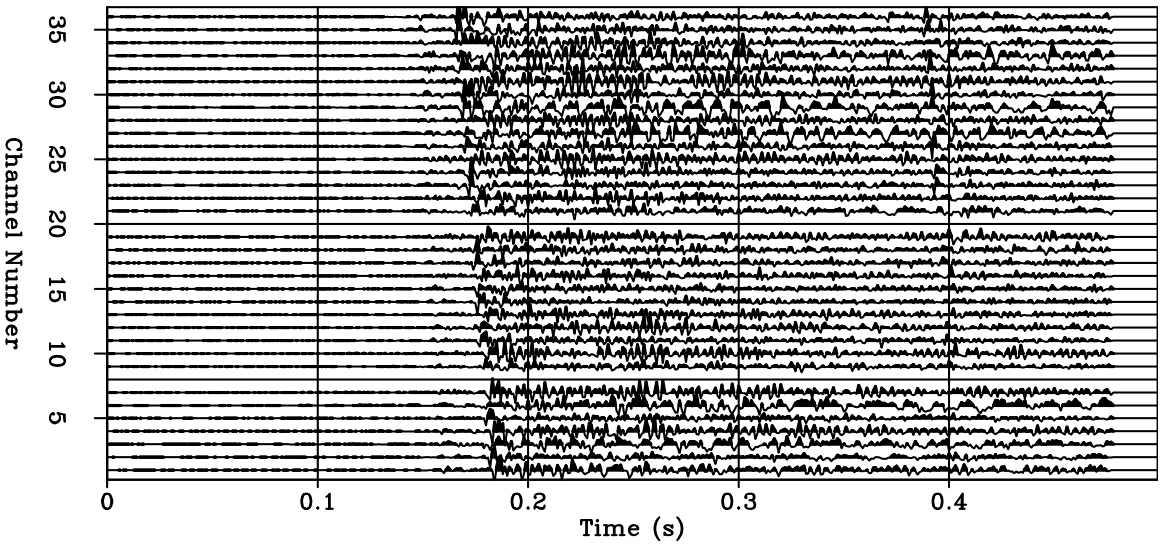

Figure 9: One of the seismograms used in making the stack in Figure 7 showing the S reflection. [**ER**]

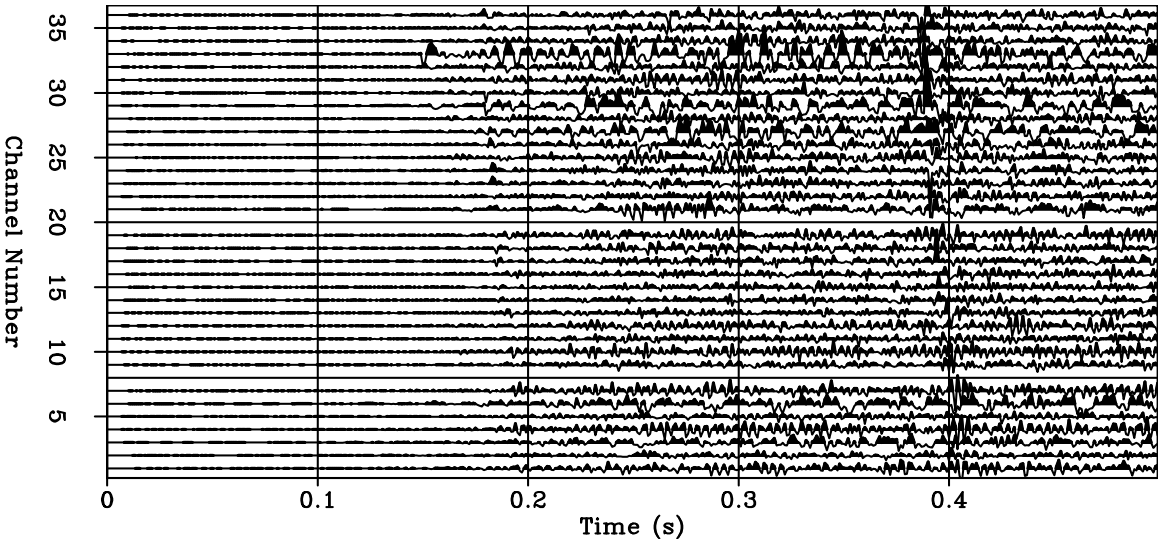

Figure 10: One of the seismograms used in making the stack in Figure 7 showing the S reflection. [**ER**]

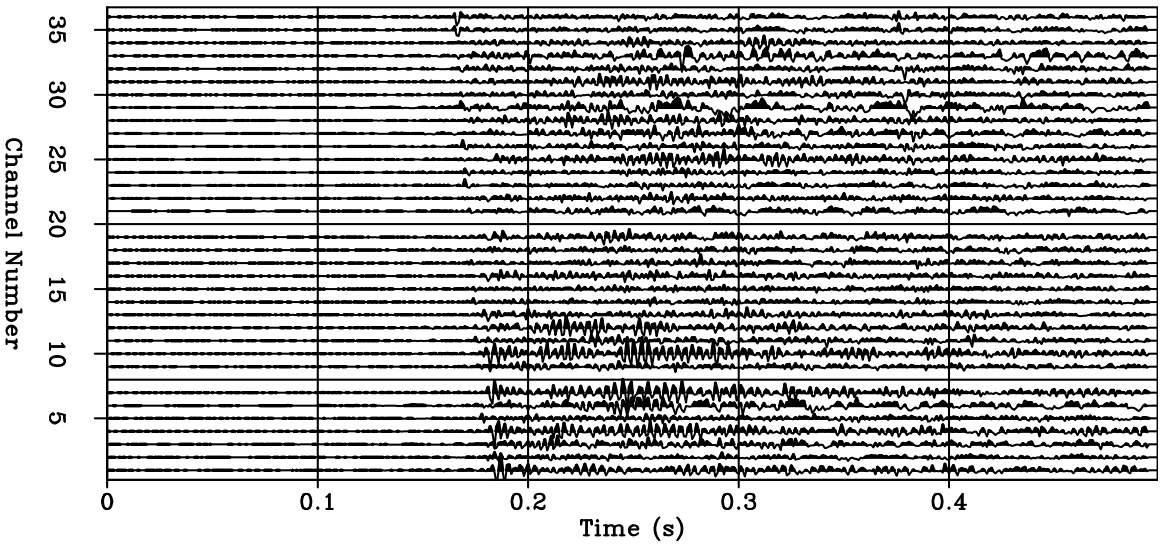

Figure 11: One of the seismograms used in making the stack in Figure 7 showing the S reflection. [**ER**]

We projected the stacked events using this direction vector to boost P arrivals and possibly see otherwise invisible P reflections. The result of this product is displayed in Figure 12. Comparing this figure with figure 7, we can see that this P-projection has indeed supressed the shear reflection at 0.39s. The S direct arrival was decreased in RMS by a factor of 1.5 and in maximum amplitude by a factor of 3. This projection also increased the P direct arrival RMS by a factor of 1.4.

As another example, Figures 13–19 exhibit a reflection at about 0.43s for a different master.

DISCUSSION

We identified clear multiplets which, disappointingly, when stacked did not produce reflection events as strong on the stack as they appeared on specific individual event windows. Using the velocity log in Figure 1, a back of the envelope calculation showed three deficiencies in our algorithm:

- Our bulk shifts to the nearest sample were too coarse for the majority of arrivals. We should be using fractional sample shifts.
- Our linear moveout corrections were similarly too coarse.
- The misalignment of later reflections due to small differences in the microseismic source locations is generally larger by a factor of 2 to 4 greater than that of the direct arrivals due to the longer travelpath of reflections. So we need to include time-variant alignment, i.e. warping.

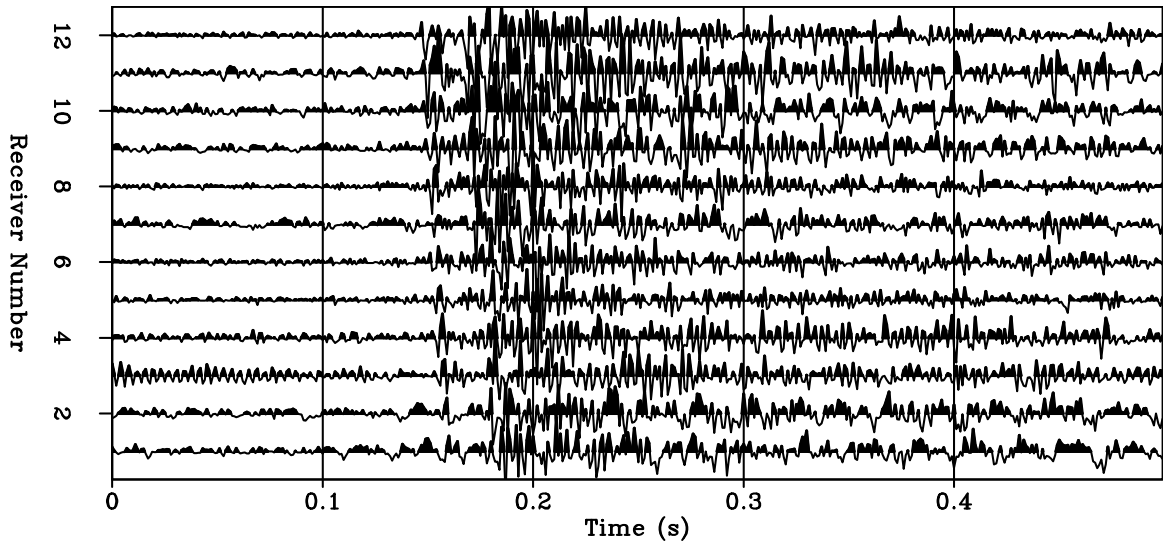

Figure 12: Stack in Figure 7 projected onto the estimated P-direction. When compared to Figure 7, reduction in S amplitude and P amplitude enhancement can be noticed. [**ER**]

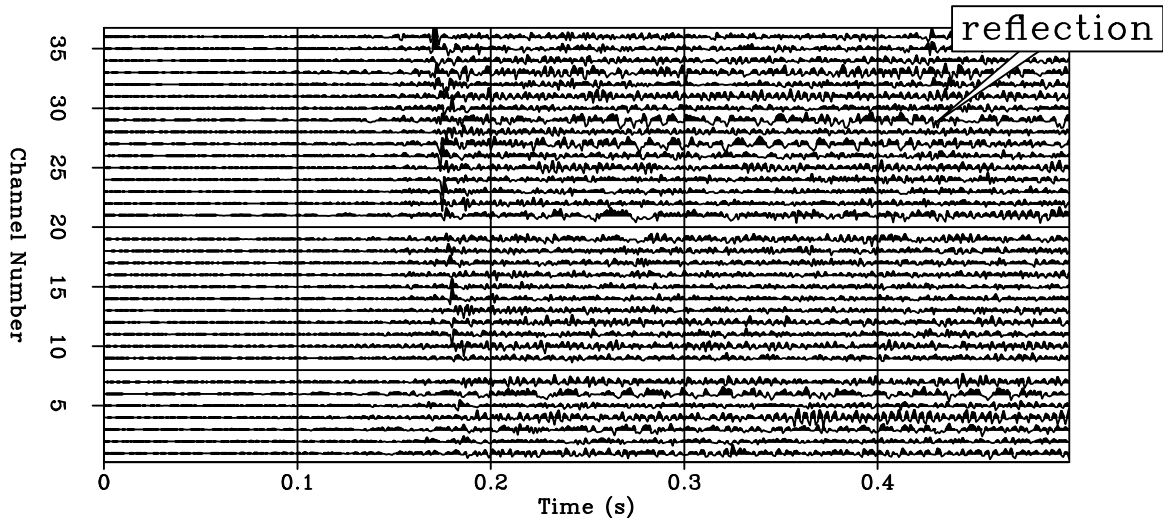

Figure 13: The stack of multiplets shown in Figure 14–19 with the S reflection marked. [**ER**]

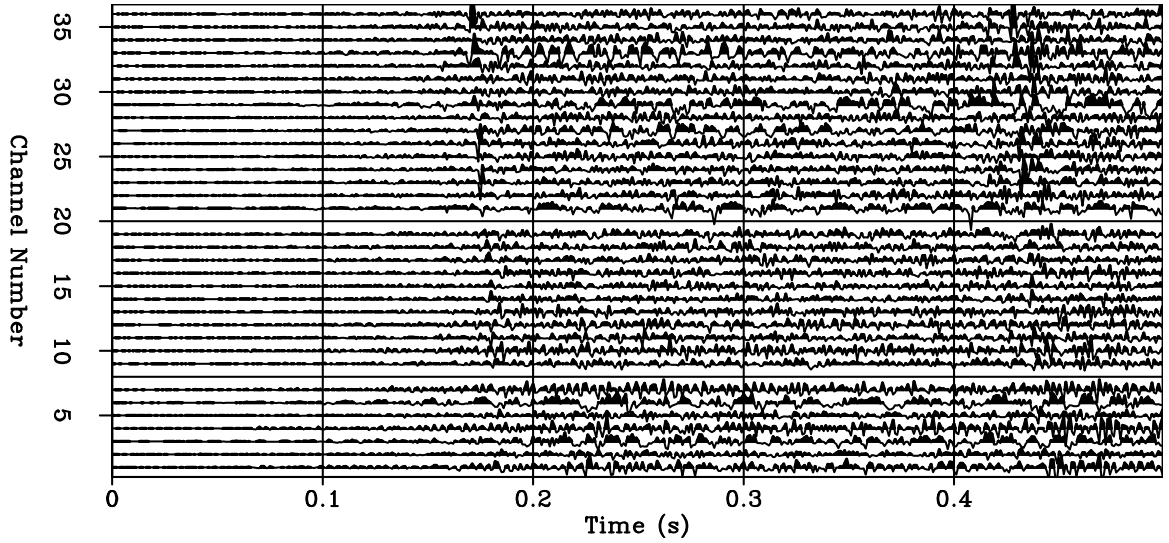

Figure 14: One of the seismograms used in making the stack in Figure 13. [**ER**]

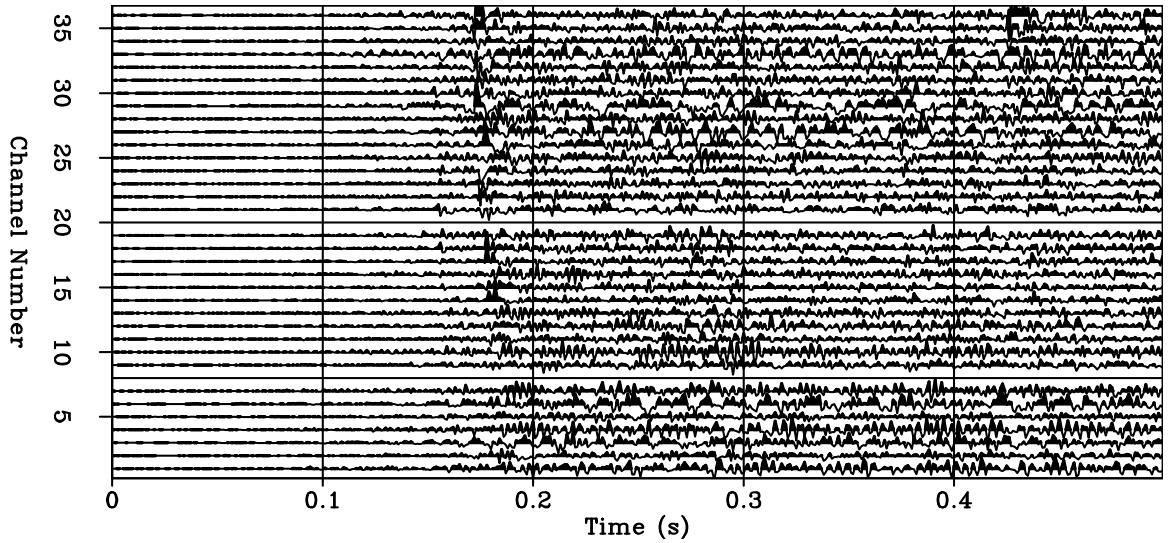

Figure 15: One of the seismograms used in making the stack in Figure 13. [**ER**]

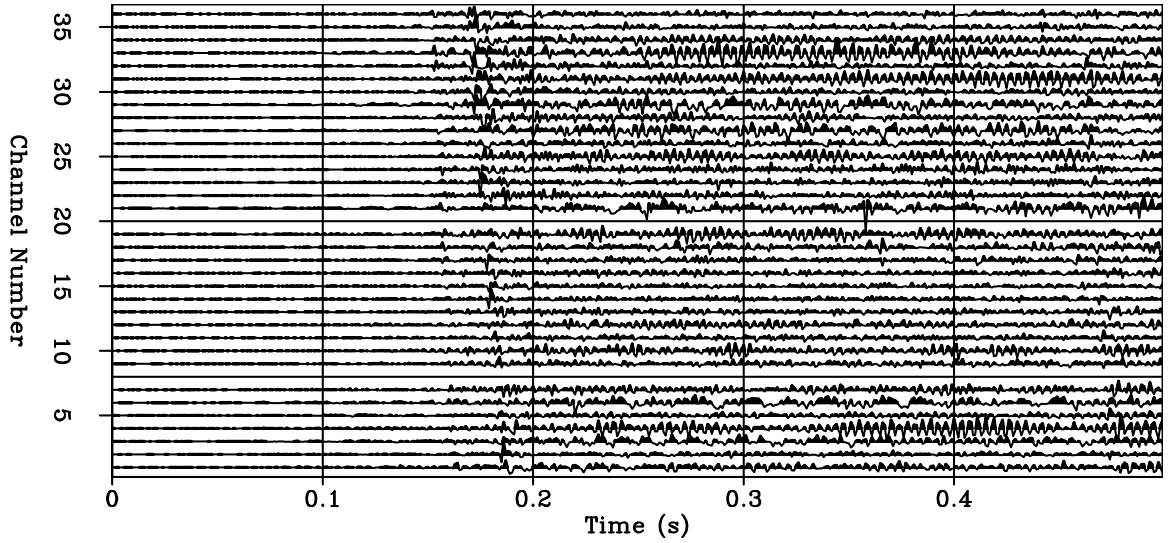

Figure 16: One of the seismograms used in making the stack in Figure 13. [**ER**]

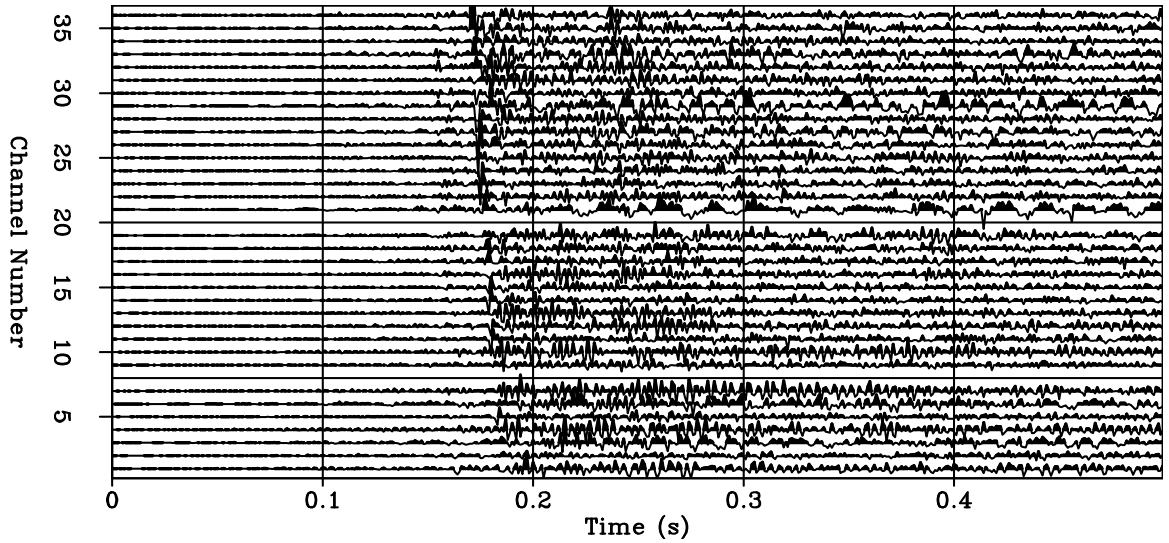

Figure 17: One of the seismograms used in making the stack in Figure 13. [**ER**]

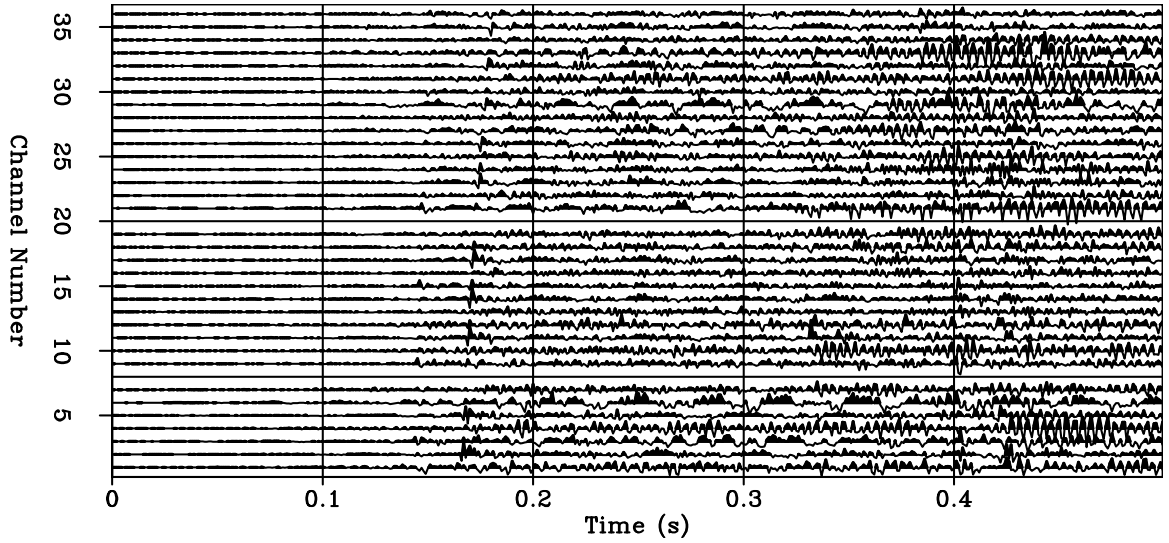

Figure 18: One of the seismograms used in making the stack in Figure 13. [**ER**]

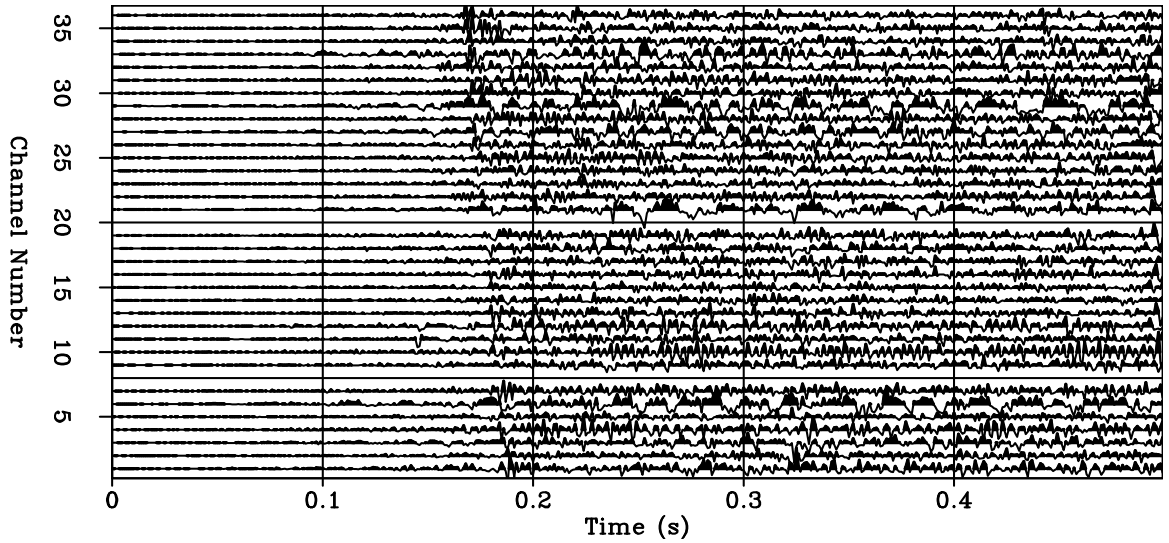

Figure 19: One of the seismograms used in making the stack in Figure 13. [**ER**]

In addition to these effects, we remark that the RMS value of the noise in the stack and the direct P-arrival have almost the same value, an additional reason why P reflections were not clearly revealed after projection even though the direct P first arrival was enhanced.

On a positive note, we can use the misalignments in reflected arrival times to constrain differences in source locations, supplementing double-difference hypocenter analysis for the microseism locations (Waldhauser and Ellsworth, 2000).

CONCLUSIONS AND FUTURE WORK

We adapted a methodology from earthquake seismology literature to identify and stack multiplets of nearly identical arrivals which successfully grouped nearly identical reflection events in the microseismic data.

However, the stacked results have been far from perfect. Stacked reflections appear to be weaker than reflections in individual event windows. This has been attributed to the fact that a trace variable shift needs to be applied to the data before stacking that is different when warping the reflection arrival from the direct arrival. Moreover, fractional rather than integer shifts need to be introduced. When such enhancement in shift precision is introduced, we hope that event windows will better stack together, enhancing the S/N ratio and boosting reflections, especially the weak P ones.

ACKNOWLEDGMENTS

We thank Pinnacle, a Halliburton company, and the United States Department of Energy for providing the dataset.

APPENDIX A

Singular value polarization analysis

Since S first arrivals are clearer and stronger than P first arrivals, we use S arrivals to estimate a vector in the general direction of P arrivals. The idea is to find the direction most perpendicular to the strongest (direct) S arrivals. We setup a $3 \times n$ matrix of shear first arrivals, $\mathbf{W}$, by windowing around the first shear arrival. As we seek a vector v that is perpendicular to the shear arrival direction (which is a P-arrival) we want

$$\mathbf{Wv} \approx \mathbf{0} \quad . \tag{A-1}$$

We solve this by minimizing the objective function

$$J = \| \mathbf{v^T W^T W v} \|_\mathbf{2} \tag{A-2}$$

subject to the constraint

$$\mathbf{v^T v} = \mathbf{1} \quad . \tag{A-3}$$

Let α and β be two spherical surface coordinate parameters over which we will minimize. Taking partial derivatives of the constraints yields:

$$\mathbf{v^T} \frac{\partial \mathbf{v}}{\partial \alpha} = \mathbf{0} \tag{A-4}$$

and

$$\mathbf{v^T} \frac{\partial \mathbf{v}}{\partial \beta} = \mathbf{0} \quad , \tag{A-5}$$

which says that $\mathbf{v^T}$ is perpendicular to the two partial derivatives. Next, taking partial derivatives of the sum of squares expression gives

$$\mathbf{v^T W^T W} \frac{\partial \mathbf{v}}{\partial \alpha} = \mathbf{0} \tag{A-6}$$

and

$$\mathbf{v^T W^T W} \frac{\partial \mathbf{v}}{\partial \beta} = \mathbf{0} \quad . \tag{A-7}$$

Therefore $\mathbf{v^T W^T W}$ is also perpendicular to both partial derivatives and consequently must be parallel to $\mathbf{v^T}$. This means that

$$\mathbf{v^T W^T W} = \lambda \mathbf{v^T} \quad , \tag{A-8}$$

where λ is the eigenvalue of the matrix $\mathbf{W}^T\mathbf{W}$ that will make the least squares expression a minimum. Transposing we get

$$\mathbf{W}^T\mathbf{W}\mathbf{v} = \lambda \mathbf{v} \quad , \tag{A-9}$$

which is a classic eigenvector problem for the matrix $\mathbf{W}^T\mathbf{W}$. Since the right singular vectors of $\mathbf{W}$ are the same as the eigenvectors of $\mathbf{W}^T\mathbf{W}$, we used the LAPACK routine *SGESVD* to find our desired P-wave direction vector.

REFERENCES

Asanuma, H., K. Tamakwa, H. Niitsuma, N. Soma, J. Rutledge, and C. Rowe, 2011, Reflection imaging of the Aneth CCS reservoir using microseismic multiplet sources: SEG Technical Program Expanded Abstracts, **30**, 1478–1482.

Brown, J. R., G. C. Beroza, and D. R. Shelly, 2008, An autocorrelation method to detect low frequency earthquakes within tremor: Geophysical Research Letters, **35**, L16305.

Eisner, L., D. Abbott, W. B. Barker, J. Lakings, and M. P. Thornton, 2008, Noise suppression for detection and location of microseismic events using a matched filter: SEG Technical Program Expanded Abstracts, **27**, 1431–1435.

Reshetnikov, A., S. Buske, and S. A. Shapiro, 2009, Active seismic imaging using microseismic events: SEG Technical Program Expanded Abstracts, **28**, 1668–1672.

Sharma, M. M., P. B. Gadde, R. Sullivan, R. Sigal, R. Fielder, D. Copeland, L. Griffin, and L. Weijers, 2008, Slick water and hybrid fracs in the Bossier: Some lessons learnt: SPE Annual Technical Conference and Exhibition, Houston, TX, USA, 89876–MS.

Shelly, D. R., Z. Peng, D. P. Hill, and C. Aiken, 2011, Triggered creep as a possible mechanism for delayed dynamic triggering of tremor and earthquakes: Nature Geoscience Letters, **4**, 384–388.

Tamakawa, K., H. Asanuma, H. Niitsuma, and N. Soma, 2010, Reflection imaging using microseismic multiplets as a source: SEG Technical Program Expanded Abstracts, **29**, 2166–2170.

Waldhauser, F. and W. L. Ellsworth, 2000, A double-difference earthquake location algorithm: Method and application to the Northern Hayward Fault, California: Bulletin of the Seismological Society of America, **90**, 1353–1368.